Hyperbaric oxygen therapy augments ciprofloxacin effect against *Pseudomonas aeruginosa* biofilm infected chronic wounds in a mouse model

Anne Sofie Laulund [a,*], Franziska Angelika Schwartz [a], Lars Christophersen [b], Mette Kolpen [a], Peter Østrup Jensen [c], Henrik Calum [d], Niels Høiby [c], Kim Thomsen [e], Claus Moser [a]

[a] *Department of Clinical Microbiology, Copenhagen University, Rigshospitalet, Denmark*
[b] *Gubra, Hørsholm Kongevej 11, B, 2970, Hørsholm, Denmark*
[c] *Department of Clinical Microbiology, Copenhagen University Hospital, Rigshospitalet and Department of Immunology and Microbiology (ISIM), University of Copenhagen, Denmark*
[d] *Department of Clinical Microbiology, Hvidovre Hospital, Denmark*
[e] *Department of Clinical Microbiology, Zealand University Hospital, Denmark*

A B S T R A C T

Introduction: Chronic wounds have a compromised microcirculation which leads to restricted gas exchange. The majority of these hypoxic wounds is infested with microorganisms congregating in biofilms which further hinders the antibiotic function. We speculate whether this process can be counteracted by hyperbaric oxygen therapy (HBOT).
Methodology: Twenty-eight BALB/c mice with third-degree burns were included in the analyses. *Pseudomonas aeruginosa* embedded in seaweed alginate beads was injected under the eschar to mimic a biofilm infected wound. Challenged mice were randomized to receive either 4 days with 1 x ciprofloxacin combined with 2×90 min HBOT at 2.8 standard atmosphere daily, 1 x ciprofloxacin as monotherapy or saline as placebo. The mice were clinically scored, and wound sizes were estimated by planimetry daily. Euthanasia was performed on day 8. Wounds were surgically removed *in toto*, homogenized and plated for quantitative bacteriology. Homogenate supernatants were used for cytokine analysis.
Results: *P. aeruginosa* was present in all wounds at euthanasia. A significant lower bacterial load was seen in the HBOT group compared to either the monotherapy ciprofloxacin group ($p = 0.0008$), or the placebo group ($p < 0.0001$). IL-1β level was significantly lower in the HBOT group compared to the placebo group ($p = 0.0007$). Both treatment groups had higher osteopontin levels than the placebo group ($p = 0.002$ and $p = 0.004$). The same pattern was seen in the S100A9 analysis ($p = 0.01$ and $p = 0.008$), whereas no differences were detected between the S100A8, the VEGF or the MMP8 levels in the three groups.
Conclusion: These findings show that HBOT improves the bactericidal activity of ciprofloxacin against *P. aeruginosa* wound biofilm *in vivo*. HBOT in addition to ciprofloxacin also modulates the host response to a less inflammatory phenotype.

1. Introduction

Temporary hypoxia immediately after wound establishment is a necessary trigger for the initiation of the healing cascade. However, healing is dependent on a subsequent reestablishment of the vascular system for sufficient tissue oxygenation. The compromised microcirculation in a chronic wound is caused by a low perfusion pressure and a low transcutaneous oxygen (O_2) tension ($TcPO_2$) of 5–20 mmHg in pathologic state compared to 30–50 mmHg in healthy tissue [1]. The hypoxic microenvironment is thought to be associated with the accumulation of necrotic tissue, waste products, edema, and hindered granulation. Many separate factors are involved in the dynamics and are contributing to this unfavorable microenvironment [2–4]. These include the altered vascular- and innate immune response caused by

comorbidities and decreased O_2-dependent defense, such as the polymorphonuclear neutrophils' (PMNs') ability to perform the respiratory burst [5–11].

P. aeruginosa is an opportunistic pathogen in burn- and chronic wounds [12–14]. It is thought to prolong the inflammatory phase of healing by displaying various virulence factors and surface proteins in addition to inducing the host response [15]. When the PMNs respond to the bacteria congregated in biofilm they release reactive O_2 species (ROS) and matrix metalloproteases (MMPs) responsible for the degradation and dislodging of the wound matrix. MMPs hydrolyze peptide bonds and must be balanced with tissue inhibitors of metalloproteinases (TIMPs) to optimize tissue remodeling. When the biofilm persists, a prolonged MMP exposure results in collateral damage of the adjacent healthy tissue [16]. The result is a prolonged inflammatory phase, an

---

* Corresponding author.
 E-mail address: annesofielaulund@gmail.com (A.S. Laulund).

inappropriate PMN- and growth factor function, damaged tissue, and increased available nutrients for the bacteria originating from the lysed cells.

The slow bacterial growth in the biofilm may contribute to prolonged antibiotic selection pressure and increased mutation rates, resulting in antibiotic tolerance, prolonged inflammation or antibiotic resistance [17,18]. The structure and composition of the wound debris combined with the biofilm extracellular matrix (EPS) acts as a physical barrier against infiltration by fibroblasts, keratinocytes and immune cells. The antibiotics are bound in the matrix, preventing them from reaching sufficient concentrations in the wound bed. The antibiotic penetration can further be limited by an underlying condition, such as diabetes, arteriosclerosis or edema. This hindered antibiotic delivery results in a concentration below the minimal inhibitory concentration (MIC) and minimal bactericidal concentration (MBC). In addition to a low antibiotic concentration in the target tissue, the O_2 depletion in the environment further limits the activity of some antibiotics [19].

Diverse approaches to counteract this complex pathologic state are being explored. This includes additional insight into the hypoxia-inducible factors (HIFs), the key players in O_2 homeostasis, new drug delivery systems with targeted or stimuli-triggered release, small molecule drugs and the optimization of either topical therapy [20–22] or hyperbaric O_2 therapy (HBOT).

A HBOT chamber can increase the dissolved plasma O_2 concentration in blood from 0.3 mL/dL at 1.0 atm to 6 mL/dL at 3.0 atm. The increased O_2 concentration moderates the ischemia-reperfusion-induced leukocyte influx, augments the neutrophil bactericidal activity, inhibits the bacterial- and improves the fibroblast-proliferation, angiogenesis and wound healing. The effects are mediated by ROS and nitrogen species generated locally in the tissue [23–27].

Using our mouse model of a chronic *P. aeruginosa* biofilm wound infection, we investigated whether adjunctive HBOT could augment the antibacterial effect of ciprofloxacin and moderate the host response.

2. Method

2.1. Mouse model and study design

Our chronic wound model is approved by the Danish animal welfare legislation (permission no. 2020-15-0201-00535).

Female 11-week-old BALB/c mice (n = 64) were purchased from Janvier Labs (Rte. du Genest, 53,940 Le Genest-Saint-Isle, France). A pilot study with 32 mice was conducted prior to the experiment to construct a valid setup. Here, mice were treated with 3 days of HBOT instead of 4 days which was applied in the current setup. All other methodology was the same in the pilot and in the current study.

Mice were acclimatized for 7 days in the rodent facility at the Biotech Research & Innovation Centre, University of Copenhagen. On day 3 of acclimatization, Nutella (Imported by Ferrero, Malmø, Sweden) was administered to assure that the mice were accustomed to taste and smell. On day 7, buprenorphine hydrochloride glucose monohydrate (Indivior Europe Limited, Dublin, Ireland) was added to the Nutella (0.3 mg/g) and 125 mg Nutella/buprenorphine mix was administered per mouse in individually ventilated cages. On day 8 (after arrival in facility), mice were shaved on their backs and prepared for the burn procedure.

The burn procedure was performed under general anesthesia ((250 μL Hypnorm (fentanylcitrat, 78.75 μg/ml; fluanisone, 2.5 mg/ml, VetaPharma Ltd, Leeds, UK) combined with midazolam (1.25 mg/ml, Accord Healthcare AB, Solna, Sweden)). A customized fire protective garment and plate was used to cover the mouse except for a 1.5×1.5 cm exposed lumbar region of the mouse. The pre-heated hot air gun was aimed at exposed skin for 5 s at a fixed distance of 4 cm. After the procedure, all mice were administered 1 mL NaCl in the cervical subcutis to avoid dehydration and single-caged. Cages were placed on 37 °C heat mats to avoid hypothermia. Easily accessible pre-watered chow, regular chow, water, Nutella with buprenorphine and cage enrichment

articles (tunnels/toys) were placed in each cage. Mice were administered an additional first dosage buprenorphine (0.1 mg/kg subcutaneously (s.c.)) after anesthesia. All following buprenorphine doses were administered orally in the Nutella. After 24 h, the cages were moved into regular individually ventilated racks and the mice were clinically evaluated daily.

On the 4th day after the burn procedure, 100 μL of 10^7 colony forming units (CFU) *P. aeruginosa* PAO1 embedded in alginate beads was injected under the eschar of all animals (Fig. 1).

2.2. Bacterial bead preparation

The alginate beads were prepared a day prior to installation under the eschar by mixing sterile filtered 1% alginate (Protanal LF 10/60 (IMCD, Helsingør, Denmark) in 0.9% salinewith a 2-times diluted overnight culture of PAO1 in lysogeny broth. The mixture was then administered through a nozzle attached to a drip counter (Gaseby3100 Syringe Pump, 20 mL/h) into a magnetic stirring (300 rpm) Tris hydrochloric acid (HCL) buffering agent with added calcium chloride. The solution was then filtered, centrifuged and beads were finally washed (x3) in a saline and calcium chloride solution. Beads were resuspended and plated for initial quantitative bacteriology. Beads were stored at 4 °C overnight.

On the day of installation, CFU were counted and the alginate suspension was diluted to reach 10^7 CFU/mL [28].

2.3. Hyperbaric oxygen therapy (HBOT)

Twenty-four hours after bead installation (day 5), the animals were anesthetized with 250 μL a cocktail of hyporm (fentanylcitrat, 78.75 μg/ml; fluanisone, 2.5 mg/ml) combined with midazolam (1.25 mg/ml) and allocated randomly to three groups.

Group I) HBOT 2 × 90 min/day plus slow acclimatization/de-acclimatization (15 minuts of each) and 500 μL Ciprofloxacin x 1 daily (0.5 mL, 2 mg/mL Fresenius Kabi, Copenhagen, Denmark) (n = 11)
Group II) 500 μL Ciprofloxacin x 1 daily (n = 11)
Group III) 500 μL saline x 1 daily, placebo group (n = 10)

All antibiotic injections (or placebo) were administered subcutaneously in the abdomen once daily. The first dosing was 24 h after infection establishment. The dosage was chosen to be suboptimal for *P. aeruginosa* eradication based on an initial study testing different dosages in our model to ensure a substantial, but not complete bacterial killing.

HBOT was executed in an Oxycom 250 ARC chamber (Hypcom, Tampere, Finland) at 2.8 bar with 100% O_2 and appropriate ventilation. The mice were sedated and placed on a preheated mat using a water-circulating heating system at 37 °C (Julebo FL 300, Buch Holm). Interventions continued for 4 consecutive days. Mice were euthanized the following day (day 8).

2.4. Clinical score

Mice were clinically scored by two scientists daily, both appearance and behavior were evaluated [29]. Groups were blinded to the investigators scoring the animals. A third scientist kept track of scores and cages.

2.5. Wound healing

Photo documentation of the wound was performed daily. Size of the wound was analyzed by two independent scientists using the free software ImageJ from the National Institutes of Health, University of Wisconsin.
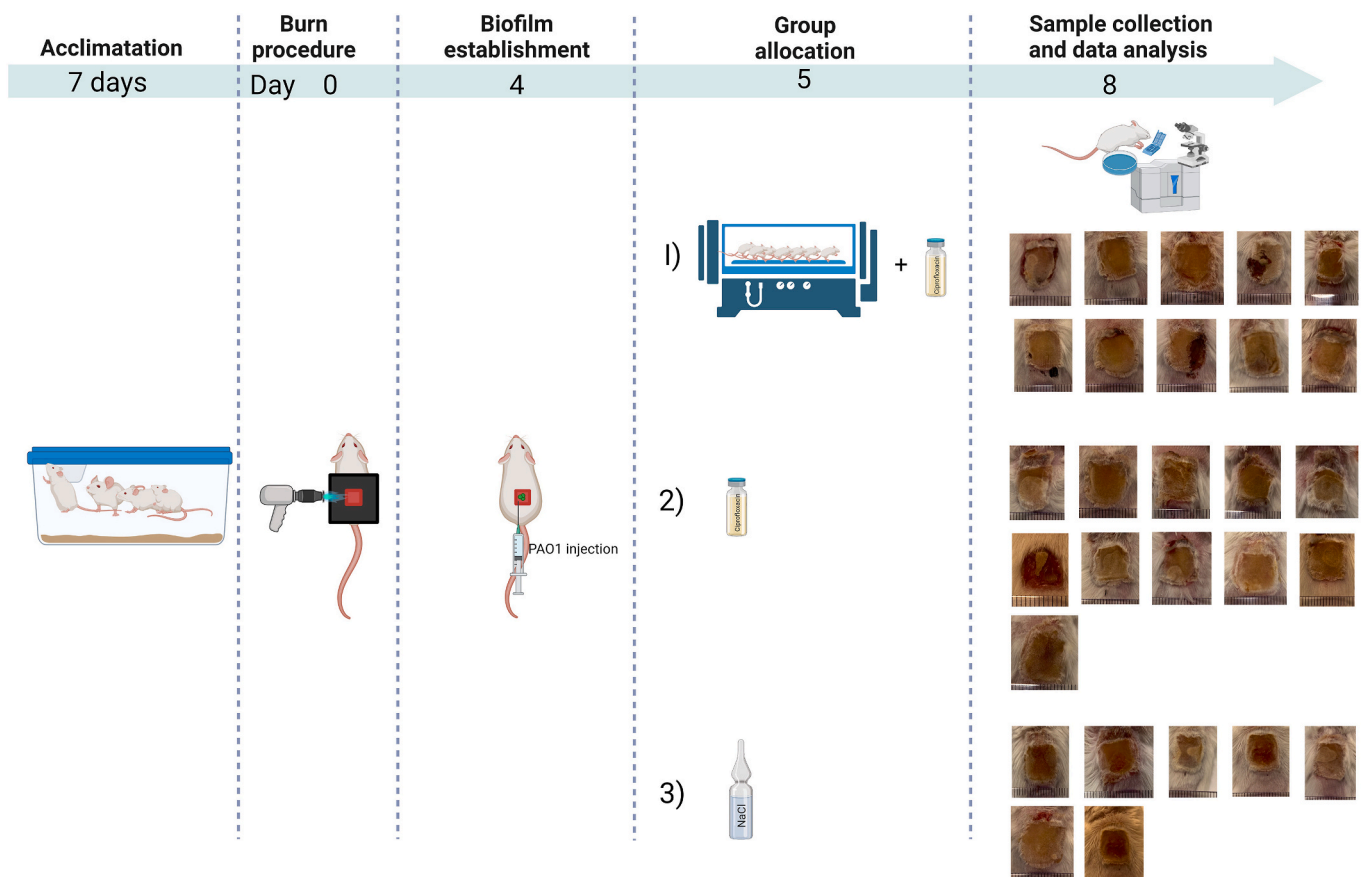
Fig. 1. Experimental setup (created with biorender.com)
32 acclimatized mice were given a full thickness necrosis on the lumbar region under general anesthesia. Post-procedure s. c. injections with saline and IVC cages with easily accessible Nutella/buprenorphine, pre-watered chow and heat were allotted to avoid pain, hypothermia and dehydration. *P. aeruginosa* embedded in seaweed alginate beads was injected under the eschar to mimic a biofilm infected wound. Mice were randomized to receive either ciprofloxacin combined with 2 × 90 min HBOT at 2.8 atm. daily (n = 10), ciprofloxacin as monotherapy (n = 11) or placebo (n = 7) for 4 consecutive days (4 mice were excluded from the study due to unexpected death or as a humane endpoint). Mice were clinically scored, and wound sizes were estimated by planimetry. Euthanasia was performed day 8. Wounds were surgically removed *in toto*, homogenized and plated for quantitative bacteriology. Homogenate supernatants were used for cytokine analysis.

2.6. Quantitative bacteriology

Postmortem, the wounds were aseptically obtained *in toto*. The wounds were placed into 2 mL microcentrifuge tubes (Nerbe plus, Winsen/Luhe, Germany) containing five glass beads and 500 mL saline. The wounds were homogenized (TissueLyser II; Qiagen, Copenhagen, Denmark) for 30 min at a frequency of 30/s. The wound homogenates were diluted in saline, plated on lactose agar plates (SSI Diagnostics, Hillerød, Denmark), incubated overnight and the CFU were counted the next day for quantitative bacteriology.

2.7. Cytokine and protease analyses

Cytokines were analyzed on the LUMINEX 200TM platform (Luminex Corp., Austin, TX, USA). The bead-based multiplex assays (Biotechne R&D Systems, Minneapolis, MN, USA) included measurements of IL-1β, S100A8, S100A9, Osteopontin (OPN), vascular endothelial growth factor (VEGF) and matrix metalloprotease-8 (MMP8).

2.8. Statistical analyses

Statistical analysis of data was performed with GraphPad Software (La Jolla, CA, USA). Data are presented as medians ± 95% confidence intervals. Differences between the groups were calculated with Kruskal–Wallis test. The level of significance was set to p = 0.05.

3. Results

From the original 32 mice of the present study, 28 were included in the statistical analyses. One mouse died during the recovery period after the burn procedure. One mouse died during the first HBOT treatment. Two mice from the placebo group were euthanized on day 3 and 4 due to reaching the humane endpoints according to the clinical scoring system.

3.1. Clinical scores, weight and wound planimetry

No statistical differences were detected when comparing the weight changes of the mice from day 0 till sacrifice day between groups (HBOT + Cipro: +0.3 g (−1.3;2.6), Cipro: −1.1 g (−2.8;1.0), Placebo: −0.9 g (−4.0;5.5), p = 0.5) nor when analyzing the clinical scores between inter- or intra-groups (figures not shown).

Comparing the wound sizes between groups on the sacrifice day did not reveal any differences (Fig. 6).

3.1.1. Quantitative bacteriology

Quantitative bacteriology revealed significant differences between the three groups (p < 0.0001) (Fig. 2). The group treated with both ciprofloxacin and adjunctive HBOT had lower bacteriology than the ciprofloxacin treated group (p = 0.0008) and both intervention groups differed significantly from the placebo group (p < 0.0001 for both).
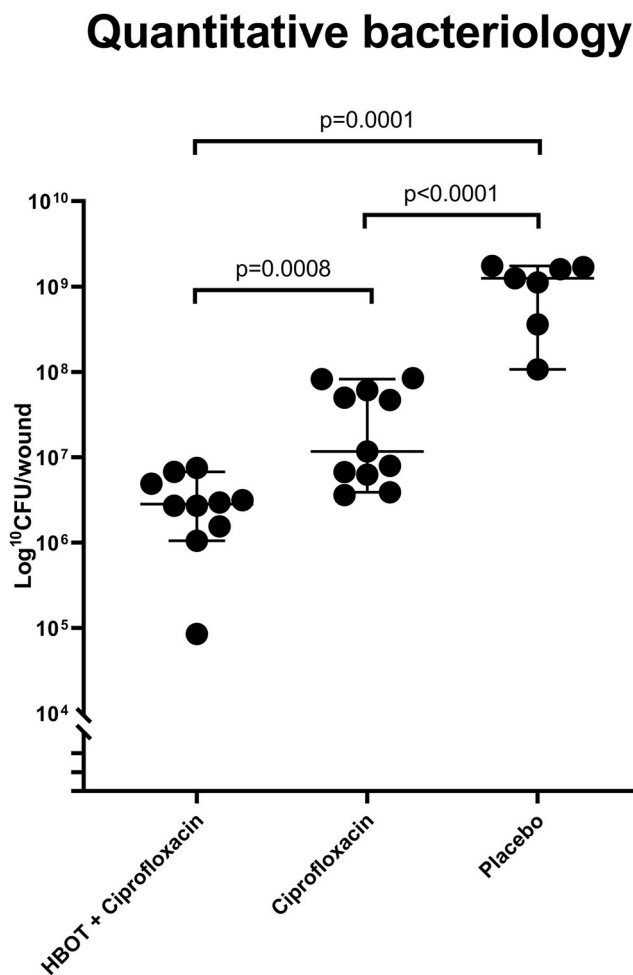
Quantitative bacteriology

IL-1b

Kruskal-Wallis, p=0.018

Fig. 3. Interleukin-1 beta is reduced in the double treated group
When the groups were compared only the group treated with both HBOT and ciprofloxacin ($3.18 \cdot 10^3$ ($2.23 \cdot 10^3; 5.44 \cdot 10^3$)) and the placebo group ($1.94 \cdot 10^4$ ($8.62 \cdot 10^3; 5.12 \cdot 10^4$)) were significantly different with a p-value of 0.0007. Data are represented as the median + 95%CI.

Fig. 2. Adjunctive HBOT reduces wound bacteriology
Quantitative bacteriology differed significantly between the three groups. The lowest median was seen in the group treated with both ciprofloxacin and adjunctive HBOT ($2.83 \cdot 10^6$ CFU/wound ($1.05 \cdot 10^6; 6.75 \cdot 10^6$)) and was significantly lower ($p < 0.0008$) than the median of the single treated group ($1.17 \cdot 10^7$ CFU/wound ($3.90 \cdot 10^6; 8.25 \cdot 10^7$)). Both intervention groups differed significantly from the placebo group ($1.25 \cdot 10^9$ CFU/wound ($1.07 \cdot 10^8; 1.74 \cdot 10^9$)) ($p \leq 0.0001$). Each data point represents the CFU in one wound. Data are represented with median and 95% confidence interval.

3.1.2. Cytokine and protease response

The wound homogenate was tested for IL-1β content (Fig. 3). The double treated group had lower IL-1β levels than the placebo group (p = 0.0007), but the IL-1β levels in the monotherapy group was not significant from the placebo group.

OPN levels were higher in both treatment groups compared to the placebo group (p = 0.002 and p = 0.004) (Fig. 4). S100A9 levels in both treatment groups were significantly higher than the level in the placebo group (p = 0.01 and p = 0.008). No significant difference was detected between the two treatment groups (Fig. 5). No significant differences in quantitated S100A8, VEGF or MMP8 between the three groups were detected (data not shown).

4. Discussion

The present project aimed at investigating the effect of HBOT as an adjuvant to ciprofloxacin in a murine chronic *P. aeruginosa* biofilm wound model. By adding HBOT, increased bacterial killing was attained by ciprofloxacin. This double intervention group showed a reduction of quantitative wound bacteriology of nearly 1 log compared to the ciprofloxacin monotherapy group and more than 2 logs compared to the
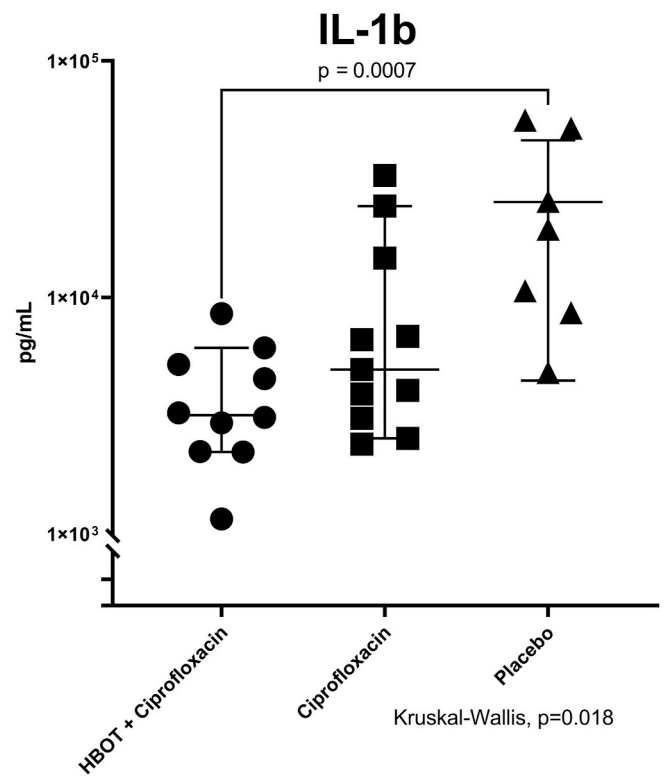
placebo treated group after 8 hyperbaric oxygen treatments in 4 days, using the same doses as used clinically for patient treatment [30]. This is in accordance with *in vitro* results, where HBOT was found to sensitize *P. aeruginosa* to antibiotics [8,9,31].

Additionally, our results showed an altered host response profile with lowered inflammation when HBOT and ciprofloxacin were administered simultaneously. Specifically, we found a lower level of the proinflammatory cytokine, IL-1β in the group of mice treated with both HBOT and ciprofloxacin compared to the control group (Fig. 3). IL-1β and HIF-1 have previously been suggested to form a signaling loop in response to hypoxia. Human and murine IL-1β genes carry multiple HIF-1-binding sites in their promoter regions, which are part of the inflammation-triggered regulation of IL-1β [32].

HIFs are known to be the key players in O_2 homeostasis. A defective HIF-1 signaling in response to local hypoxia is thought to contribute to a failed upregulation. We speculate that the supplemented extra O_2 may prevent transcription of the IL-1β genes due to the O_2-induced dislocation of HIF-1 from its binding sites. The applied HBOT was, however, insufficient to induce differences in the expression of VEGF, which is responsible for initiating angiogenesis and nitric oxide production, or failure to adapt to anaerobic metabolism and thus hindering the healing of chronic wounds regulated by HIF-1 [24,33]. Since VEGF did not reveal any differences between the groups, indicating that HIF-mediated VEGF expression was not influenced by HBOT in this setup, the unaffected expression of VEGF may in part explain the absent effect of HBOT on the wound sizes.

Osteopontin is a multipotent cytokine and is known to act on the innate and adaptive immune response. OPN activates the expression of adhesion molecules on endothelial cells and initiates recruitment as well as inhibits the apoptosis of PMNs. It is also known to be involved in pathology, where it contributes to the development of immune-
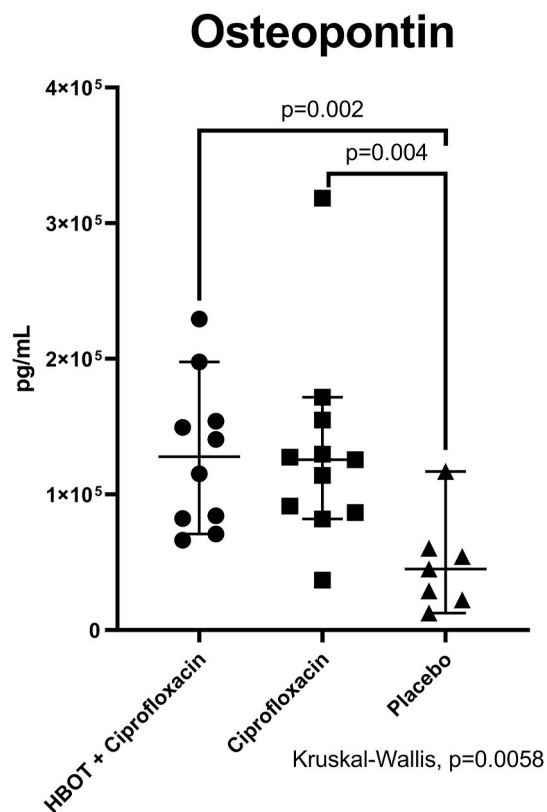
Fig. 4. Osteopontin levels are elevated in the treated groups
OPN levels were higher in both treatment groups compared to the placebo group (p = 0.002 and p = 0.004), median and 95%CI were respectively $(3.18 \cdot 10^3$ $(1.28 \cdot 10^5; 6.13 \cdot 10^5)$, $1.26 \cdot 10^5$ $(8.19 \cdot 10^4; 1.72 \cdot 10^5)$ and $4.50 \cdot 10^4$ $(1.25 \cdot 10^4; 1.17 \cdot 10^5)$. Data are represented as median + 95%CI.

mediated and inflammatory diseases [34]. In our setup, we detected higher levels of OPN in the treatment groups compared to the placebo group, but no difference between the treatment groups, which corresponds to earlier results from our group in this experimental setup [35]. OPN is primarily considered a proinflammatory protein, but also displays considerable anti-inflammatory and neovascularizing abilities [36]. Together with the lowered IL-1β levels in the double treated group, this increase in OPN is interpreted as a marker for an increased anti-inflammatory, angiogenic and anti-apoptotic- status and could thus mark a progression into the proliferative phase of wound healing [36–39].

The immune and inflammation modulatory calcium- and zinc-binding proteins, S100A8 and S100A9 were also investigated. S100 proteins are predominantly found as heterodimers and are thought to be regulated in a negative feedback loop. S100A8/A9, also known as calprotectin, has multiple intra- and extracellular functions. S100A8/A9 is a danger-associated molecular pattern molecule (DAMP) and can induce neutrophil chemotaxis and adhesion. It modulates the cytoskeleton components and neutrophilic NADPH-oxidase. S100A8/A9 also acts as an antimicrobial by chelating Zn^{2+} and prevents tissue damage by oxidant-scavenging and apoptosis-inducing functions [40–43]. We previously showed the immunomodulatory, bactericidal and resistance-preventing abilities of S100A8/A9 when administered with ciprofloxacin [35,44–47]. Our group has also previously investigated S100A8/A9 in a clinical setting, where the S100A8/A9 level was significantly reduced in wound fluid from venous ulcers compared with healing wounds [46]. Our current findings indicate that S100A8 and A9 might be differentially regulated.
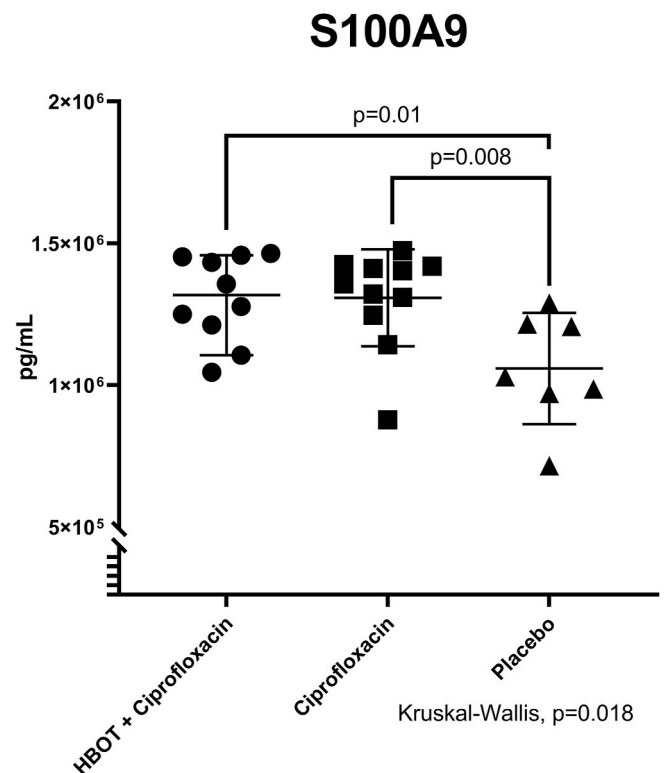

Fig. 5. S100A9 levels are elevated in the treated groups
The S100A9 levels in both the treatment groups were significantly higher than the level in the placebo group (p = 0.01 and p = 0.008 $(1.32 \cdot 10^6$ $(1.11 \cdot 10^6; 1.46 \cdot 10^6)$, $1.36 \cdot 10^6$ $(1.14 \cdot 10^6; 1.43 \cdot 10^6)$ and $1.03 \cdot 10^6$ $(7.16 \cdot 10^5; 1.29 \cdot 10^6)$). Data are represented as median and 95%CI.

4.1. Limitations of the study

Humans heal with granulation and re-epithelialization. On the basis of the *panniculus carnosus* layer in rodent's skin, the wound contracts almost immediately after injury, making a wound size difficult to evaluate in a rodent wound model. Indeed, wound sizes did not show any difference in the present study and were only considered a secondary endpoint. Though HBOT significantly enforced the bactericidal effect of ciprofloxacin, the absent effects on wound healing may indicate that the remaining bacterial population in all groups were too large to allow progression into the proliferative phase of wound healing. Further studies involving additional reduction of the bacterial population by longer periods of treatment are thus warranted for the possible detection of increased wound healing by adjuvant HBOT. Despite this difference, the translational relevance of murine models in chronic wound research is prominent in order to identify feasible adjunctive treatments to be further investigated.

5. Conclusion

Our findings show that HBOT improves the bactericidal activity of ciprofloxacin on *P. aeruginosa* biofilm *in vivo* in a chronic wound infection mouse model. HBOT in addition to ciprofloxacin modulates the host response to a more anti-inflammatory phenotype.

Since HBOT is already approved for human use in the same doses as used here, our results could justify establishing a clinical study of adjunctive HBOT in the management of non-healing wounds.

CRediT authorship contribution statement

Anne Sofie Laulund: Conceptualization, Formal analysis, Writing –
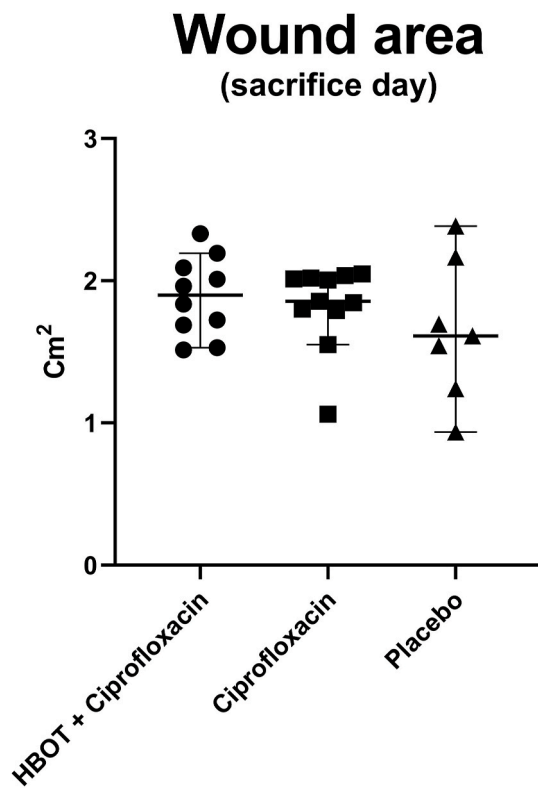
Wound area
(sacrifice day)

Fig. 6. Wound sizes on sacrifice day were not significantly different between the groups. The group receiving both HBOT and ciprofloxacin had a wound area of 1.9 cm^2 (1.5;2.2), the group receiving ciprofloxacin had an area of 1.9 cm^2 (1.6;2.04) and the placebo group had a wound size of 1.6 mm^2 (0.9;2.39), p = 0.6). Data are represented as median and 95%CI.

original draft, ideation with conception and design of the study, laboratory work, Data analysis, interpretation, Drafting of manuscript, revisions. **Franziska Angelika Schwartz:** Conceptualization, ideation with conception and design of the study, laboratory work, interpretation, revisions. **Lars Christophersen:** Conceptualization, ideation with conception and design of the study, laboratory work, interpretation, revisions. **Mette Kolpen:** Conceptualization, ideation with conception and design of the study, interpretation, revisions. **Peter Østrup Jensen:** Conceptualization, ideation with conception and design of the study, interpretation, revisions. **Henrik Calum:** Conceptualization, ideation with conception and design of the study, interpretation, revisions. **Niels Høiby:** Conceptualization, ideation with conception and design of the study, interpretation, revisions. **Kim Thomsen:** Conceptualization, ideation with conception and design of the study, interpretation, revisions. **Claus Moser:** Conceptualization, Writing – original draft, ideation with conception and design of the study, interpretation, Drafting of manuscript, revisions. All authors contributed significantly to the work.

Declaration of competing interest

Data availability

Data will be made available on request.

References

[1] Tandara AA, Mustoe TA. Oxygen in wound healing–more than a nutrient. World J Surg 2004;28:294–300. https://doi.org/10.1007/s00268-003-7400-2.

[2] Woo KY, Brandys TM, Marin JA. Assessing chronic wound perfusion in the lower extremity: current and emerging approaches. CWCMR 2015;2:149–57. https://doi.org/10.2147/CWCMR.S60326.

[3] Heng MC, Harker J, Csathy G, Marshall C, Brazier J, Sumampong S, et al. Angiogenesis in necrotic ulcers treated with hyperbaric oxygen. Ostomy/Wound Manag 2000;46:18–28. 30–2.

[4] Gottrup F, Dissemond J, Baines C, Frykberg R, Jensen PØ, Kot J, et al. Use of oxygen therapies in wound healing. J Wound Care 2017;26. https://doi.org/10.12968/jowc.2017.26.Sup5.S1. S1–43.

[5] Kohanski MA, Dwyer DJ, Hayete B, Lawrence CA, Collins JJ. A common mechanism of cellular death induced by bactericidal antibiotics. Cell 2007;130: 797–810. https://doi.org/10.1016/j.cell.2007.06.049.

[6] Jensen PØ, Briales A, Brochmann RP, Wang H, Kragh KN, Kolpen M, et al. Formation of hydroxyl radicals contributes to the bactericidal activity of ciprofloxacin against Pseudomonas aeruginosa biofilms. Pathog Dis 2014;70: 440–3. https://doi.org/10.1111/2049-632X.12120.

[7] Walters MC, Roe F, Bugnicourt A, Franklin MJ, Stewart PS. Contributions of antibiotic penetration, oxygen limitation, and low metabolic activity to tolerance of Pseudomonas aeruginosa biofilms to ciprofloxacin and tobramycin. Antimicrob Agents Chemother 2003;47:317–23.

[8] Kolpen M, Lerche CJ, Kragh KN, Sams T, Koren K, Jensen AS, et al. Hyperbaric oxygen sensitizes anoxic Pseudomonas aeruginosa biofilm to ciprofloxacin. Antimicrob Agents Chemother 2017;61. https://doi.org/10.1128/AAC.01024-17.

[9] Kolpen M, Mousavi N, Sams T, Bjarnsholt T, Ciofu O, Moser C, et al. Reinforcement of the bactericidal effect of ciprofloxacin on Pseudomonas aeruginosa biofilm by hyperbaric oxygen treatment. INT J ANTIMICROB AG 2016;47:163–7. https://doi.org/10.1016/j.ijantimicag.2015.12.005.

[10] Gill AL, Bell CNA. Hyperbaric oxygen: its uses, mechanisms of action and outcomes. QJM 2004;97:385–95. https://doi.org/10.1093/qjmed/hch074.

[11] Stewart PS, Costerton JW. Antibiotic resistance of bacteria in biofilms. Lancet 2001;358:135–8.

[12] Gjødsbøl K, Christensen JJ, Karlsmark T, Jørgensen B, Klein BM, Krogfelt KA. Multiple bacterial species reside in chronic wounds: a longitudinal study. Int Wound J 2006;3:225–31. https://doi.org/10.1111/j.1742-481X.2006.00159.x.

[13] Raizman R, Little W, Smith AC. Rapid diagnosis of Pseudomonas aeruginosa in wounds with point-of-care fluorescence imaing. Diagnostics 2021;11:280. https://doi.org/10.3390/diagnostics11020280.

[14] Estahbanati HK, Kashani PP, Ghanaatpisheh F. Frequency of Pseudomonas aeruginosa serotypes in burn wound infections and their resistance to antibiotics. Burns 2002;28:340–8. https://doi.org/10.1016/S0305-4179(02)00024-4.

[15] Serra R, Grande R, Butrico L, Rossi A, Settimio U, Caroleo B, et al. Chronic wound infections: the role of Pseudomonas aeruginosa and Staphylococcus aureus. Expert Rev Anti-infect Ther 2015;13:1–9. https://doi.org/10.1586/14787210.2015.1023291.

[16] Caley MP, Martins VLC, O'Toole EA. Metalloproteinases and wound healing. Adv Wound Care 2015;4:225–34. https://doi.org/10.1089/wound.2014.0581.

[17] Uruén C, Chopo-Escuin G, Tommassen J, Mainar-Jaime RC, Arenas J. Biofilms as promoters of bacterial antibiotic resistance and tolerance. Antibiotics 2020;10:3. https://doi.org/10.3390/antibiotics10010003.

[18] Ciofu O, Moser C, Jensen PØ, Høiby N. Tolerance and resistance of microbial biofilms. Nat Rev Microbiol 2022;20:621–35. https://doi.org/10.1038/s41579-022-00682-4.

[19] Li H, Zhou X, Huang Y, Liao B, Cheng L, Ren B. Reactive oxygen species in pathogen clearance: the killing mechanisms, the adaption response, and the side effects. Front Microbiol 2021;11.

[20] Nataraj M, Maiya AG, Karkada G, Hande M, Rodrigues GS, Shenoy R, et al. Application of topical oxygen therapy in healing dynamics of diabetic foot ulcers - a systematic review. Rev Diabet Stud 2019;15:74–82. https://doi.org/10.1900/RDS.2019.15.74.

[21] Rg F, Pj F, M E, Jn B, L T, T W, et al. A multinational, multicenter, randomized, double-blinded, placebo-controlled trial to evaluate the efficacy of cyclical topical wound oxygen (TWO2) therapy in the treatment of chronic diabetic foot ulcers: the TWO2 study. Diabetes Care 2019;43:616–24. https://doi.org/10.2337/dc19-0476.

[22] Rayman G, Vas P, Dhatariya K, Driver V, Hartemann A, Londahl M, et al. Guidelines on use of interventions to enhance healing of chronic foot ulcers in diabetes (IWGDF 2019 update). Diabetes Metabol Res Rev 2020;36. https://doi.org/10.1002/dmrr.3283.

[23] Wattel F, Mathieu D, Nevière R, Bocquillon N. Acute peripheral ischaemia and compartment syndromes: a role for hyperbaric oxygenation. Anaesthesia 1998;53 (Suppl 2):63–5. https://doi.org/10.1111/j.1365-2044.1998.tb15161.x.

[24] Hong WX, Hu MS, Esquivel M, Liang GY, Rennert RC, McArdle A, et al. The role of hypoxia-inducible factor in wound healing. Adv Wound Care 2014;3:390–9. https://doi.org/10.1089/wound.2013.0520.

[25] Thangarajah H, Vial IN, Grogan RH, Yao D, Shi Y, Januszyk M, et al. HIF-1 alpha dysfunction in diabetes. Cell Cycle 2010;9:75–9. https://doi.org/10.4161/cc.9.1.10371.

[26] Marx RE, Ehler WJ, Tayapongsak P, Pierce LW. Relationship of oxygen dose to angiogenesis induction in irradiated tissue. Am J Surg 1990;160:519–24. https://doi.org/10.1016/s0002-9610(05)81019-0.

[27] de Wolde SD, Hulskes RH, de Jonge SW, Hollmann MW, van Hulst RA, Weenink RP, et al. The effect of hyperbaric oxygen therapy on markers of oxidative stress and the immune response in healthy volunteers. Front Physiol 2022;13.

[28] Christophersen LJ, Trøstrup H, Malling Damlund DS, Bjarnsholt T, Thomsen K, Jensen PØ, et al. Bead-size directed distribution of Pseudomonas aeruginosa results in distinct inflammatory response in a mouse model of chronic lung infection. Clin Exp Immunol 2012;170:222–30. https://doi.org/10.1111/j.1365-2249.2012.04652.x.

[29] Fentener van Vlissingen J, Borrens M, Girod A, Lelovas P, Morrison F, Torres YS. The reporting of clinical signs in laboratory animals: FELASA Working Group Report. Lab Anim 2015;49:267–83. https://doi.org/10.1177/0023677215584249.

[30] Kranke P, Bennett MH, Martyn-St James M, Schnabel A, Debus SE, Weibel S. Hyperbaric oxygen therapy for chronic wounds. Cochrane Database Syst Rev 2015; 2015. https://doi.org/10.1002/14651858.CD004123.pub4.

[31] Gade P, Olsen T, Jensen PØ, Kolpen M, Høiby N, Henneberg K-Å, et al. Modelling of ciprofloxacin killing enhanced by hyperbaric oxygen treatment in Pseudomonas aeruginosa PAO1 biofilms. PLoS One 2018;13:e0198909. https://doi.org/10.1371/journal.pone.0198909.

[32] Zhang W, Petrovic J-M, Callaghan D, Jones A, Cui H, Howlett C, et al. Evidence that hypoxia-inducible factor-1 (HIF-1) mediates transcriptional activation of interleukin-1β (IL-1β) in astrocyte cultures. J Neuroimmunol 2006;174:63–73. https://doi.org/10.1016/j.jneuroim.2006.01.014.

[33] Jb W. Physiological effects of chronic hypoxia. N Engl J Med 2017;376. https://doi.org/10.1056/NEJMra1612008.

[34] Clemente N, Raineri D, Cappellano G, Boggio E, Favero F, Soluri MF, et al. Osteopontin bridging innate and adaptive immunity in autoimmune diseases. J Immunol Res 2016;2016:7675437. https://doi.org/10.1155/2016/7675437.

[35] Laulund AS, Schwartz F, Trøstrup H, Thomsen K, Christophersen L, Calum H, et al. Adjunctive S100A8/A9 immunomodulation hinders ciprofloxacin resistance in *Pseudomonas aeruginosa* in a murine biofilm wound model. Front Cell Infect Microbiol. 2021 Apr 12;11:652012. https://doi.org/10.3389/fcimb.2021.652012. PMID: 33912476; PMCID: PMC8072475.

[36] Wang W, Li P, Li W, Jiang J, Cui Y, Li S, et al. Osteopontin activates mesenchymal stem cells to repair skin wound. PLoS One 2017;12:e0185346. https://doi.org/10.1371/journal.pone.0185346.

[37] Mazzali M, Kipari T, Ophascharoensuk V, Wesson JA, Johnson R, Hughes J. Osteopontin–a molecule for all seasons. QJM 2002;95:3–13. https://doi.org/10.1093/qjmed/95.1.3.

[38] Icer MA, Gezmen-Karadag M. The multiple functions and mechanisms of osteopontin. Clin Biochem 2018;59:17–24. https://doi.org/10.1016/j.clinbiochem.2018.07.003.

[39] Buback F, Renkl AC, Schulz G, Weiss JM. Osteopontin and the skin: multiple emerging roles in cutaneous biology and pathology. Exp Dermatol 2009;18:750–9. https://doi.org/10.1111/j.1600-0625.2009.00926.x.

[40] Ghavami S, Kerkhoff C, Los M, Hashemi M, Sorg C, Karami-Tehrani F. Mechanism of apoptosis induced by S100A8/A9 in colon cancer cell lines: the role of ROS and the effect of metal ions. J Leukoc Biol 2004;76:169–75. https://doi.org/10.1189/jlb.0903435.

[41] Sroussi HY, Williams RL, Zhang QL, Villines D, Marucha PT. Ala42S100A8 ameliorates psychological-stress impaired cutaneous wound healing. Brain Behav Immun 2009;23:755–9. https://doi.org/10.1016/j.bbi.2009.03.006.

[42] Viemann D, Strey A, Janning A, Jurk K, Klimmek K, Vogl T, et al. Myeloid-related proteins 8 and 14 induce a specific inflammatory response in human microvascular endothelial cells. Blood 2005;105:2955–62. https://doi.org/10.1182/blood-2004-07-2520.

[43] Koike A, Arai S, Yamada S, Nagae A, Saita N, Itoh H, et al. Dynamic mobility of immunological cells expressing S100A8 and S100A9 in vivo: a variety of functional roles of the two proteins as regulators in acute inflammatory reaction. Inflammation 2012;35:409–19. https://doi.org/10.1007/s10753-011-9330-8.

[44] Laulund ASB, Trøstrup H, Lerche CJ, Thomsen K, Christophersen L, Calum H, et al. Synergistic effect of immunomodulatory S100A8/A9 and ciprofloxacin against Pseudomonas aeruginosa biofilm in a murine chronic wound model. Pathog Dis 2019. https://doi.org/10.1093/femspd/ftz027.

[45] Trøstrup H, Lerche CJ, Christophersen L, Jensen PØ, Høiby N, Moser C. Immune modulating topical S100a8/A9 inhibits growth of Pseudomonas aeruginosa and mitigates biofilm infection in chronic wounds. Int J Mol Sci 2017;18. https://doi.org/10.3390/ijms18071359.

[46] Trøstrup H, Lundquist R, Christensen LH, Jorgensen LN, Karlsmark T, Haab BB, et al. S100A8/A9 deficiency in nonhealing venous leg ulcers uncovered by multiplexed antibody microarray profiling. Br J Dermatol 2011;165:292–301. https://doi.org/10.1111/j.1365-2133.2011.10384.x.

[47] Trøstrup H, Holstein P, Christophersen L, Jørgensen B, Karlsmark T, Høiby N, et al. S100A8/A9 is an important host defence mediator in neuropathic foot ulcers in patients with type 2 diabetes mellitus. Arch Dermatol Res 2016;308:347–55. https://doi.org/10.1007/s00403-016-1646-7.